Agrociencia

ARTIFICIAL NEURAL NETWORK MODELS FOR PREDICTION OF STANDARDIZED PRECIPITATION INDEX IN CENTRAL MEXICO

Rafael **Magallanes-Quintanar**[1], Carlos Eric **Galván-Tejada**[1], Jorge Issac **Galván-Tejada**[1], Santiago de Jesús **Méndez-Gallegos**[2], Fidel **Blanco-Macías**[3], Ricardo David **Valdez-Cepeda**[3*]

[1] Universidad Autónoma de Zacatecas. Unidad Académica de Ingeniería Eléctrica. Av. Ramón López Velarde No. 801, Centro, Zacatecas, Zacatecas, México. C. P. 98000.
[2] Colegio de Posgraduados Campus San Luis Potosí. Iturbide No. 73, Salinas de Hidalgo, San Luis Potosí, México. C. P. 78600.
[3] Universidad Autónoma Chapingo. Centro Regional Universitario Centro Norte. Cruz del Sur No. 100, Col. Constelación, El Orito, Zacatecas, Zacatecas, México. C. P. 98085.
* Author for correspondence: vacrida@hotmail.com

Citation: Magallanes-Quintanar R, Galván-Tejada CE, Galván-Tejada JI, Méndez-Gallegos S de J, Blanco-Macías F, Valdez-Cepeda RD. 2023. Artificial neural network models for prediction of standardized precipitation index in central Mexico. **Agrociencia** https://doi.org/ 10.47163/agrociencia.v57i1.2655

Editor in Chief:
Dr. Fernando C. Gómez Merino

Received: March 02, 2022.
Approved: December 30, 2022.
Published in Agrociencia: February 10, 2023.

ABSTRACT

Globally, an increase in the occurrence of droughts may be due to the effects of climate change on rainfall patterns. Drought prediction based on historical rainfall behavior can be very useful in sectors where water is a critical element, such as rain-fed agriculture. Therefore, drought classification and characterization based on drought index prediction models could aid in mitigating their negative effects in such water-sensitive sectors. The primary goal of this paper was to test a Multilayer Perceptron Artificial Neural Network as a model to forecast the monthly Standardized Precipitation Index in north-central México using rainfall data from the 1964–2014 period. The model was obtained using the Hyperbolic Tangent activation function and the optimization method from the Adaptive Moment Estimation algorithm. The model used a 26-12-1 network architecture with 4 weights and 365 trainable parameters. The scatter plot analysis between predicted and observed Standardized Precipitation Index values for the test dataset resulted in a Coefficient of Determination between 0.84 and 0.88. Based on quantitative statistics averaged across the test set, the Artificial Network Model performed substantially well in predicting the Standardized Precipitation Index at the four studied regions. This was confirmed by an all-region average value of the performance statistics Mean Absolute Error (0.081), Mean Square Error (0.014) and the Coefficient of Determination (0.867). We conclude that the Artificial Network models developed and tested in this research provided adequate monthly Standardized Precipitation Index skills for the analyzed stations in the studied territory.

Key words: Drought, rainfall, artificial intelligence, SPI.

INTRODUCTION

The vulnerability of human activities to extreme events such as floods and droughts due to changes in rainfall distribution and intensity is an important research topic (Kharin *et al*., 2007; Angheluţă and Badea, 2015). A meteorological drought occurs when the observed precipitation is less than the long-term average (Choubin *et al*., 2016). Droughts have a significant negative effect because they reduce freshwater

flows, which has a great impact on water resource planning and management (Ali *et al*., 2017). There have been numerous approaches proposed to estimate droughts. Drought indices are some of the most extensively used methods. McKee *et al*. (1993) developed the Standardized Precipitation Index (SPI) to categorize observed rainfall as a standardized deviation from a rainfall probability distribution function.

In recent years, SPI has been used as a method for climatic zone classification and as a drought indicator, allowing for comparisons to be made in space and time (Naresh Kumar *et al*., 2009). Because this index only uses records of precipitation data over time, it has a significant advantage over other indices due to its ease of calculation and temporal flexibility. Mahfouz *et al*. (2016) found that SPI has the potential to be used for monitoring drought conditions in forestry and agriculture in Lebanon. Giddings *et al*. (2005) used SPI to establish dynamically consistent precipitation zones throughout Mexico. However, SPI can be used to define much smaller and more detailed areas. Magallanes-Quintanar *et al*. (2019) used it to organize monthly time series from the state of Zacatecas in Mexico into small groups with similar regional precipitation regimes. The current trends suggest less than median precipitation across the state of Zacatecas. Nevertheless, SPI forecasts for the near future have been little studied, so they remain practically unknown. This type of information could be essential to adjust the activities of the inhabitants based on planned drought adaptation strategies.

Recently, models have also been developed not only for assessment but also drought forecasting. Although, historically, time series of meteorological variables such as monthly precipitation and temperature have been extensively modeled using linear techniques such as autoregressive moving average (ARMA) and seasonal autoregressive integrated moving average (SARIMA), it should be noted that the use of artificial intelligence (AI) models has shown good performance and accuracy in drought forecasting. A neural network is an information processing method which determines patterns from data in an adaptive manner (Ali *et al*., 2017).

Specifically, much research in recent years has focused in the use of Artificial Neural Network (ANN) models as a useful data-driven tool for drought index forecasting. Ozger *et al*. (2011) developed a wavelet fuzzy logic model to estimate a Drought Severity Index. The SPI was predicted using an ARIMA model and matched to machine learning approaches such as ANNs by Belayneh *et al*. (2014). Masinde (2014) used a blend of ANN and Effective Drought Index as a drought forecasting approach. Deo and Şahin (2015) analyzed the feasibility of the ANN as a data-driven model to forecast the monthly SPI. Choubin *et al*. (2016) applied several data-driven techniques to predict SPI. Ali *et al*. (2017) used a multilayer perceptron neural network algorithm for drought forecasting and Soh *et al*. (2018) worked with a Wavelet-ARIMA-ANN model and the latest Wavelet-Adaptive Neuro-Fuzzy Inference System model to predict the SPI.

Since Multilayer Perceptron neural network model (MLP) is one of the leading types of ANN's methods for modeling hydrological data (Ali *et al*., 2017), the approach in this study was to develop a MLP Network model over a 50-year period (1964–2014) in

central Mexico, aiming to: (a) predict regional Standardized Precipitation Index, and (b) forecast regional Standardized Precipitation Index for 12 months (near future).

MATERIALS AND METHODS

Precipitation data

The regional time series of Standardized Precipitation Index assessed by Magallanes-Quintanar *et al*. (2019) were obtained from a database of long-term records (50 years, 1964–2014) of monthly precipitation acquired at 31 weather stations located within the territory of the Mexican state of Zacatecas (Figure 1). The database was provided by the Mexican National Water Commission (CONAGUA). All datasets were inspected for missing values and outliers.

Standardized Precipitation Index

McKee *et al*. (1993) defined the Standardized Precipitation Index (SPI) as the number of standard deviations that observed cumulative precipitation deviates from the climatological mean. The SPI was developed mainly for specifying and monitoring droughts. As presented by Koudahe *et al*. (2017), the SPI is computed as follows:
A gamma function using monthly rainfall data is defined as:

$$g(x) = \frac{1}{\beta^{\alpha}\Gamma(\alpha)} x^{\alpha-1} e^{\frac{-x}{\beta}}$$

for $x > 0$.

The density probability function $g(x)$, has α as a shape parameter ($\alpha > 0$), β as a scale parameter ($\beta > 0$), and

$$\Gamma(\alpha) = \int_0^{\alpha} y^{\alpha-1} e^{-1} dy$$

where $\Gamma(\alpha)$ is the gamma function.

The parameters α and β are calculated by means of:

$$\alpha = \frac{1}{4A}\left(1 + \sqrt{1 + \frac{4A}{3}}\right)$$

$$\beta = \frac{x}{a}$$

$$A = ln(\overline{x}) - \frac{\sum ln(\overline{x})}{n}$$

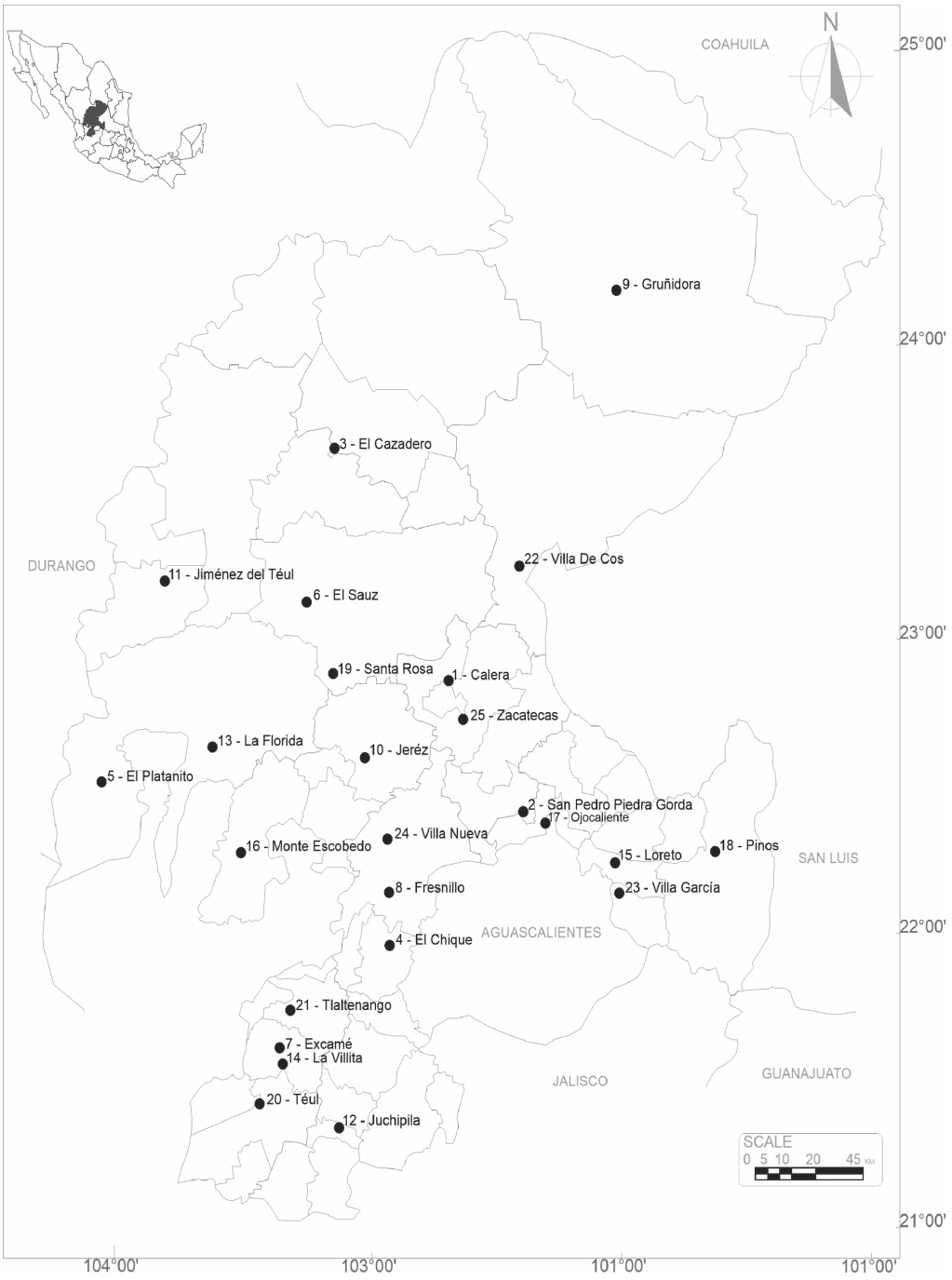

Figure 1. Study region of the Zacatecas state territory in Mexico and the location of weather stations.

where n is the number of rainfall observations and $\overline{x}$ is the arithmetic mean over a time scale. A cumulative probability $G(x)$ of an observed volume of rainfall per each month and time scale (if α and β estimators were used to integrate the probability density function with respect to x) is calculated as follows:

$$G(x) = \int_0^x g(x)dx = \frac{1}{\overline{\beta}^{\overline{\alpha}}\Gamma(\overline{\alpha})}\int_0^x x^{\overline{\alpha}} e^{\frac{\overline{x}}{\overline{\beta}}} dx$$

When substituting t for $\frac{\overline{x}}{\overline{\beta}}$ in the preceding equation, the result is the incomplete gamma function:

$$G(x) = \frac{1}{\Gamma(\overline{\alpha})}\int_0^x t^{\overline{\alpha}-1} e^{-1}\, dt$$

Nevertheless, the gamma distribution function is undefined for $x = 0$ and $q = P(x = 0) > 0$; where $P(x = 0)$ is the probability of zero precipitation. Thus, the actual probability of non-exceedance $H(x)$ should be calculated as follows (Edwards and McKee, 1997; Usman *et al*., 2014):

$$H(x) = q + (1 - q)G(x)$$

Where $H(x)$ is the actual probability of non-exceedance and q the probability of $x = 0$. If m is the number of zeros in a rainfall time series sample of size n, then q is assessed as:

$$q = \frac{m}{n}$$

Lastly, to calculate the SPI, the cumulative probability distribution $H(x)$ is standardized to a normal variable $Z \sim N(0,1)$. The SPI results can be interpreted as wet or drought periods as pointed out by McKee *et al*. (1993).

Several time scales can be used to calculate the SPI, with changes in rainfall affecting different aspects of the hydrological cycle (Koudahe *et al*., 2017). As pointed out by Caloiero (2017), the 6-month SPI describes droughts that affect plant life and agriculture, whereas the 12-month SPI describes droughts that can affect water supplies/reserves. In this study, we evaluated the SPI on a 12-month time scale.

Due to the difficulty of manually calculating the SPI, several computer programs have been developed to solve this task. One of the most widely used programs is the one developed by the United States National Drought Mitigation Centre. The program 'SPIGenerator' is freely available at http://drought.unl.edu/droughtmonitoring/SPI/SPIProgram.aspx. In this research we used the R system 4.0.2 (R Core Team, 2020)

and the 'SPEI' package (Beguería and Vicente-Serrano, 2013) for SPI estimation. Both are freely available at the Comprehensive R Archive Network (https://www.cran.r-project.org/).

The interannual comparison for SPI estimated values at timescale of 12 months for each region are shown (Figure 2).

Neural Network Forecasting

The Artificial Neural Network (ANN) models can identify the nonlinear relationships between the input and output data using computational paradigms that attempt to represent the brain neural connections (McCulloch and Pits, 1943). To forecast climatological time series, ANN models have been used successfully. Among them, the Multilayer Perceptron (MLP) Network is one of the most widely used ANN approaches to model hydrological information (Wang *et al*., 2006; Ali *et al*., 2017). It has been proven that ANN could be a more efficient alternative than traditional methods for modeling time-series with non-linear behavior (Farajzadeh *et al*., 2014).

A simple artificial neural network is the feed-forward neural network. In this kind of ANN, the information is processed in one direction trough the hidden nodes and does not form a cycle. The structure of the feedforward neural network includes, at least, the input layer and the number of features or variables. The first includes the neurons that receive the inputs and transmit the information to the hidden layers. The second includes the number of features or variables that must equal the number of neurons

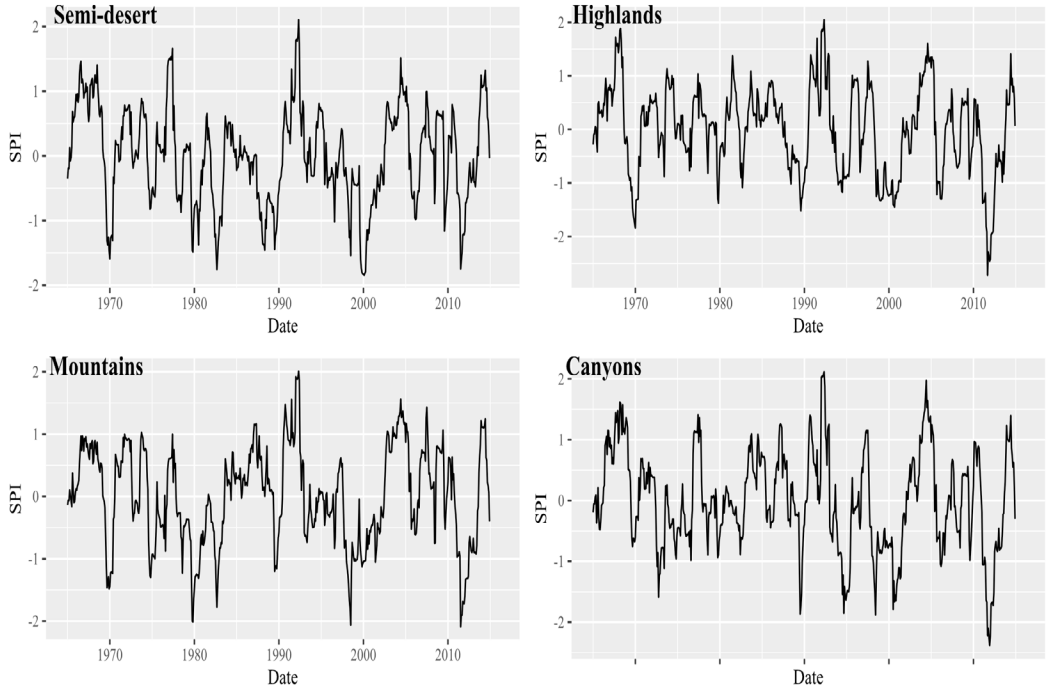

Figure 2. Regional SPI time-series at 12-month timescale for the Zacatecas state territory.

in this layer. The hidden layers are positioned between the input and output layers, they may contain a significant number of neurons which apply transformations to the input information before passing it to the next layer. As the network is trained, the weights are renewed to be more predictive. The neuron weights refer to the strength or amplitude of a connection between an input and a neuron. The forecasted feature or variable that depends on the type of examined model is represented by the output layer.

Typically, the data processing trough a feed-forward network (Figure 3) follows the next steps:

1. Multiplication of weights and inputs: The inputs are multiplied by the designated weight values.
2. Adding the biases: The result of the previous phase is added to their respective biases and the modified inputs are then summed up to acquire a single value.
3. Activation: An activation function introduces non-linear properties in the hidden layer and transfer the result to the output layer. It is called an activation/transfer function because it controls the inception at which a neuron is triggered and the strength of the output data.
4. Output signal: The weighted sum achieved in the previous phase is turned into an output signal.

In the MLP model, we suppose that there are n layers. The first layer is the input layer and the last one (n_{th}) is the output layer. Hence, the hidden layers go from 2 to n-1 layers. In this model, the neuron is the main processing unit which calculates the weighted sum of its input signals. As explained by Deo and Şahin (2015), a single neuron may be described by:

$$u_k = \sum_{j=1}^{m} w_k x_j$$

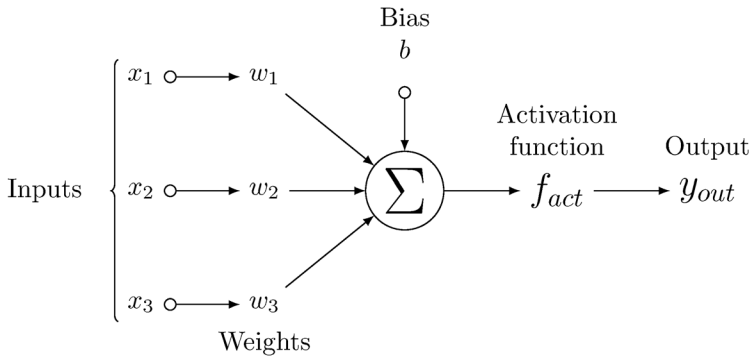

Figure 3. Neural networking pipeline diagram.

where x_1 to x_m are the input signals, and w_{k1} to w_{km} are the synaptic weights of the k neuron. The output signal of the neuron is defined as:

$$y_k = f(u_k + b_k)$$

where u_k is the linear combination output from input signals, b_k is the bias and f the activation function that could be (among others): binary step, linear, sigmoid, hyperbolic tangent, SoftMax, rectified linear unit, exponential linear units, and swish (Sharma *et al*., 2020).

Generally, neural networks have at least only one input layer and one output layer, but the number of hidden layers may differ; the selection of these variables is domain-specific or varies on the problem (Ali *et al*., 2017). Furthermore, the internal structure (inputs and hidden units) and the layout of those ANN's units are difficult to elucidate and are often established using a trial-and-error approach or established in advance from prior experience.

After the selection of variables or features, the development of a MLP starts with the training, testing, and validation of the neural network with the aim of learning. It is possible to fine-tune the network after this step by varying the architecture after this step. Once the network architecture is established, the model can be tested and verified. The final step is model forecasting.

The Python programming language is widely used in science and data analysis. Moreover, Keras and Tensor flow are approachable and highly-productive interfaces for solving machine learning problems. In this research we used the Python language version 3.85 (Python Software Foundation, https://www.python.org/) and Google's open-source machine learning framework 'TensorFlow' (Abadi *et al*., 2016). In addition, we used the high-level neural network API 'Keras' (Chollet, 2015) for fitting an ANN to 4 regional times-series (Semi-desert, Highlands, Mountains and Canyons) of SPI yielded by Magallanes-Quintanar *et al*. (2019) to forecast the SPI-12 index values in each region. Simulations were performed on an AMD Ryzen 7 processor running at 2.3 GHz.

The first 40 years of data (80 %) for each regional SPI-12 time-series (1965–2004) were used as a training dataset for the model prior to implementing the architecture model. After the selection of the appropriate parameters, SPI values were validated or tested using the remaining 20 % of data (2005–2014). As previously stated, the architecture model was determined through trial-and-error. In our case, we considered the works of Deo and Şahin (2015) and Ali *et al*. (2017) to set the MLP layout. The neural network training by means of Keras-Tensor Flow was specified to use a sequential model with Hyperbolic Tangent as activation function and Adaptative Moment Estimation as optimizer algorithm (Kingma and Ba, 2015). Additionally, we selected 1000 epochs as hyperparameter of gradient descent to control the number of passes through the time-series dataset.

The algorithm can train the network in any difficult and complex situation and offers early stopping to prevent overfitting. When evaluating ANN models, accuracy metrics or performance measures are used for comparison models. Among several performance measures or metrics, in the present research, we used the Mean Absolute Error (MAE), the Mean Square Error (MSE), and the Coefficient of Determination (R^2).

$$MAE = \frac{1}{n}\sum_{i=1}^{n}\left|\left(SPI_{p_i} - SPI_{o_i}\right)\right|$$

$$MSE = \frac{1}{n}\sum_{i=1}^{n}\left(SPI_{p_i} - SPI_{o_i}\right)^2$$

MAE is a measure of the average deviation of the predicted values from the corresponding observed values and can provide information on long term performance of the models; the lower MAE, the better is the long-term model prediction. MSE is a measure of the difference between the observed and calculated values; the lower the MSE, the more accurate the prediction is (Jierula *et al*., 2021). The last metric evaluation was the R^2 as efficiency criterion representing the percentage of the initial uncertainty explained by the model. A good model should have a lower MSE and MAE, both indicate low-accumulated errors; then, the best fit between observed and calculated values, which is unlikely to occur, would have MSE=0 and R^2=1.

Furthermore, to assess the prediction error (PE) of the model, the difference between the observed and predicted SPI values was used (Chapra and Canale, 2006):

$$PE = SPI_{o_i} - SPI_{p_i}$$

Because the MLP model encapsulates the inner characteristics of a complex process, it is possible to predict future values after defining the features or variables, establishing the model and their parameters, training and validating the model. To that end, a 12-month database was built to make SPI-12 variable predictions.

RESULTS AND DISCUSSION

The training process resulted in a 26-13-1 network architecture with 4 weights and a total of 365 trainable parameters. The above architecture includes a dense layer with shape (none, 1, 26) with 338 parameters, a flatten layer with shape (none, 26) with 0 parameters and a dense, 1 layer with shape (none, 1) with 27 parameters. The established architecture was in line with the works of Deo and Şahin (2015) who chose an architecture 18-43-1 and Ali *et al*. (2017) who selected an architecture of 30-8-1.

The ANN SPI-12 observed and predicted values for Semi-desert, Highlands, Mountains and Canyon regions are shown (Figure 4). In general, the estimated MSE

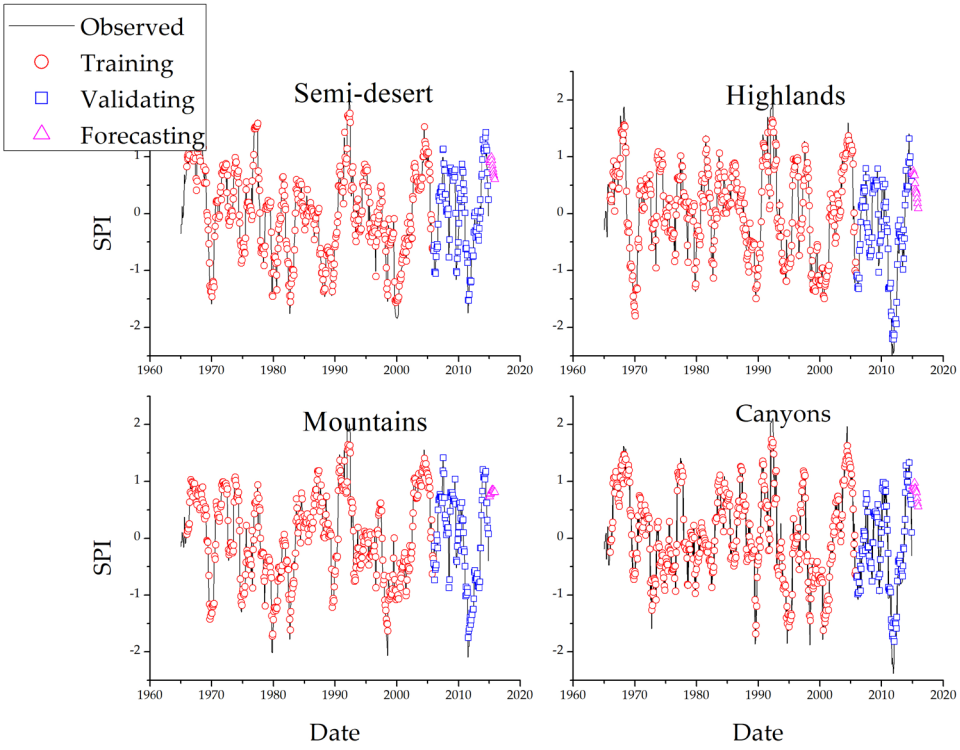

Figure 4. Observed and predicted regional SPI time-series for the Zacatecas state territory.

and MAE values were low (Table 1). Those results indicate that the 4 regional SPI model's performance were adequately accurate.

The performance of ANN models was evaluated using a scatter plot (Figure 5) and linear regression statistics for all four regions during the validation period (2005-2014) (Table 2). For the optimal ANN models at each region, *y*-intercepts (β_0) oscillated between 0.003 (Highlands region) and 0.034 (Canyons region), and the gradient of the linear fit (β_1) ranged from 0.84 (Canyons region) to 0.93 (Semi-desert region). The

Table 1. Quantitative measures of the ANN performance in validation phase for regional SPI time series for the Zacatecas State, Mexico.

Region	MSE	MAE
Semi-desert	0.015	0.082
Highlands	0.013	0.078
Mountains	0.014	0.071
Canyons	0.015	0.083

Key measures: Mean Square Error (MSE) and Mean Absolute Error (MAE).

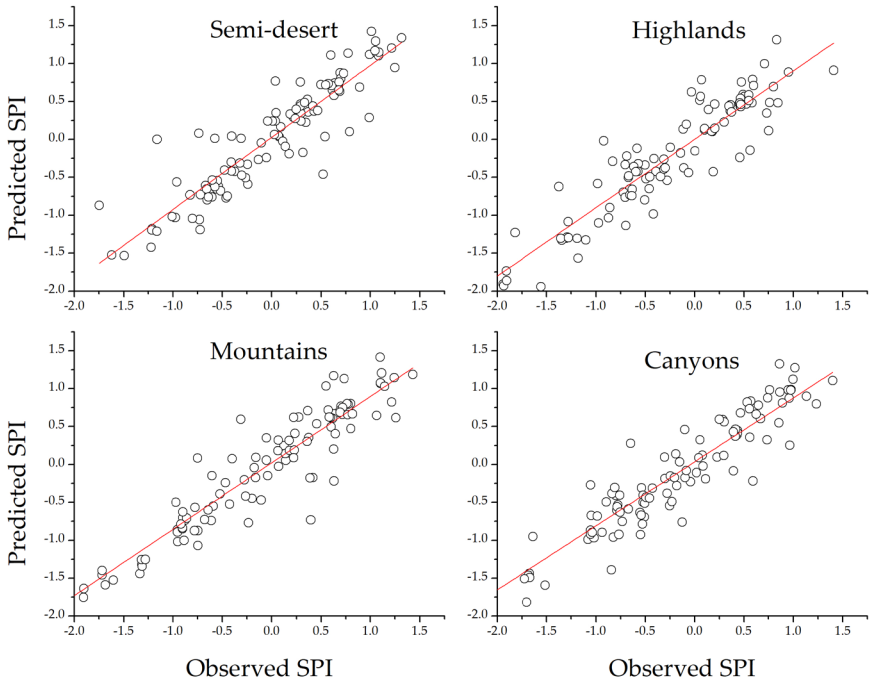

Figure 5. Correlation between the original SPI values and the predicted ANN SPI values during the validating period for regional SPI time series for the Zacatecas State, Mexico.

Table 2. Assessment of ANN model performance based on linear regression formula (SPIp = β_0 + β_1 SPIo) of observed SPI values (SPIo) and predicted SPI values (SPIp) during the validating period for regional SPI time series for the Zacatecas state, Mexico.

Region	β_0	β_1	R^2	R
Semi-desert	0.013	0.931	0.843	0.918
Highlands	0.003	0.902	0.879	0.938
Mountains	0.021	0.866	0.861	0.933
Canyons	0.034	0.844	0.878	0.937

correlation coefficient (*r*) stretched between 0.91 (Semi-desert region) and 0.93 (Canyons region). Hence, models indicated high correspondence between the predicted and the observed SPI values.

Overall, there was good visual concordance among the observed and the predicted SPI values over the 108 months during the validation period (Figure 5). This was consistent with the results pointed out by summarized statistics of the scatter plot between the predicted and the observed SPI values (Table 2). To infer the overall prediction skill of the ANN model, a contrast of its performance was achieved using the performance statistics for all months within the validation dataset by means of the MSE, MAE, and R^2 (Tables 1 and 2).

Evidence suggests that the best ANN model predictions correspond to the Highlands regions. The smallest values of both MAE (≈0.078) and MSE (≈0.013), as well as the highest R^2 (0.879), were associated to this region. The Mountains regions had the second performance, followed by the Semi-desert and Canyons regions. Moreover, the higher values of MAE and MSE correspond to the ANN model prediction for the Canyons regions.

Overall, the ANN models demonstrated good prediction skill for all study regions. The probability under normal distribution of prediction error representing under-predictions (PE < 0) and over-predictions (PE > 0) by the ANN models is shown (Table 3). In general, the under-prediction values were higher than the over-prediction values for all regions. This implies that ANN models under-predicted the SPI for all regions, with the Canyons region having the largest difference with a probability of 59.34 % and the Semi-desert region having the smallest difference with a probability of 51.71 %. On the other hand, the minimum probability value of over-prediction with 40.66 % was found for the Canyons and the maximum probability value of over-prediction error was found for the Semi-desert with 48.29 %.

Table 3. Probability under normal distribution of prediction error (PE) for observed SPI values (SPIo) and the predicted SPI values (SPIp) during the validating period for regional SPI time series for the state of Zacatecas, Mexico.

Region	PE < 0	PE > 0
Semi-desert	0.517	0.483
Highlands	0.550	0.450
Mountains	0.535	0.465
Canyons	0.593	0.407

Notably, neural networks have demonstrated to be extremely useful methods for empirically forecasting hydrological variables (Daliakopoulos *et al*., 2005; Farajzadeh *et al*., 2014). Our results are comparable with those of Deo and Şahin (2015), Ali *et al*. (2017) and Soh *et al*. (2018) who used the ANN model to forecast the monthly standardized precipitation index. Moreover, our results lend support to those of Giddings *et al*. (2005) because our approach allows for derivation of smaller and detailed regional zones in Mexico by means of the SPI.

CONCLUSIONS

Recently, drought prediction is a challenging issue in hydrology, water resources management, and rainfed agriculture, among other fields, due to the negative impacts of droughts on human activities related to water use. Multilayer perceptron models were used to predict the values of four monthly Standardized Precipitation Index (SPI) time series from the Mexican Zacatecas State. The models were trained and tested using the regional SPI time series and the output variables were the predicted by the SPI's.

After trial and error, the best network architecture was a combination of 26-13-1 as the input-hidden-output neurons based on smallest MSE and largest coefficient of determination for each region. A good agreement between observed and predicted SPI values using the scatter plot analysis and their corresponding model for each region. ANN models performed very well in predicting regional SPI values in terms of quantitative statistics over the test set.

In general, the developed and tested ANN models reflect satisfactory prediction skills of the monthly Standardized Precipitation Index for the four regional time series studied. Our study used ANN models by optimizing hidden neurons, activation functions, and several combinations of training and testing algorithms. Although our research is focused on the study of SPI-12, it is possible to use the entire framework to study SPI at different time scales. In the context of climate change, drought forecast by using ANN models as a framework in future studies would be beneficial to generate useful information for decision making. In addition, future works should evaluate a variety of input parameters besides the SPI observed values to assess the effects of different network architectures.

REFERENCES

Abadi M, Barham P, Chen J, Chen Z, Davis A, Dean J, Zheng X. 2016. Tensorflow: A system for large-scale machine learning. *In* 12th symposium on operating systems design and implementation (OSDI 16). USENIX: Savannah, GA, USA, pp: 265–283. https://www.usenix.org/system/files/conference/osdi16/osdi16-abadi.pdf (Retrieved: December 2021).

Ali Z, Hussain I, Faisal M, Nazir HM, Hussain T, Shad MY, Hussain Gani S. 2017. Forecasting drought using multilayer perceptron artificial neural network model. Advances in Meteorology 2017: 1–9. https://doi.org/10.1155/2017/5681308

Angheluţă PS, Badea CG. 2015. The water resources in the context of climate change produced by the greenhouse gases. University of Oradea, Faculty of Economics 1 (2): 637–643.

Beguería S, Vicente-Serrano SM. 2013. SPEI: Calculation of the standardized precipitation-evapotranspiration index. R Foundation for Statistical Computing. Vienna, Austria. https://www.cran.r-project.org/ (Retrieved: December 2021).

Belayneh A, Adamowski J, Khalil B, Ozga-Zielinski B. 2014. Long-term SPI drought forecasting in the Awash River Basin in Ethiopia using wavelet neural network and wavelet support vector regression models. Journal of Hydrology 508: 418–429. https://doi.org/10.1016/j.jhydrol.2013.10.052

Caloiero T. 2017. Drought analysis in New Zealand using the standardized precipitation index. Environmental Earth Sciences 76 (16): 1–13. https://doi.org/10.1007/s12665-017-6909-x

Chapra SC, Canale RP. 2006. Numerical methods for engineers. McGraw-Hill Higher Education: Boston, MA, USA. 987 p.

Chollet F. 2015. Keras. GitHub. https://github.com/fchollet/keras (Retrieved: December 2021).

Choubin B, Malekian A, Golshan M. 2016. Application of several data-driven techniques to predict a standardized precipitation index. Atmósfera 29 (2): 121–128. https://doi.org/10.20937/ATM.2016.29.02.02

Daliakopoulos IN, Coulibaly P, Tsanis IK. 2005. Groundwater level forecasting using artificial neural networks. Journal of Hydrology 309 (1–4): 229–240. https://doi.org/10.1016/j.jhydrol.2004.12.001

Deo RC, Şahin M. 2015. Application of the artificial neural network model for prediction of monthly standardized precipitation and evapotranspiration index using hydrometeorological parameters and climate indices in eastern Australia. Atmospheric Research 161: 65–81. https://doi.org/10.1016/j.atmosres.2015.03.018

Edwards DC, McKee TB. 1997. Characteristics of 20th century drought in the United States at multiple time scales. Climatology Report No. 7-2. Atmospheric Paper No. 634. 152-155. Colorado State University, Department of Atmospheric Science: Fort Collins, CO, USA. https://mountainscholar.org/handle/10217/170176. (Retrieved: December 2021).

Farajzadeh J, Fard AF, Lotfi S. 2014. Modeling of monthly rainfall and runoff of Urmia lake basin using "feed-forward neural network" and "time series analysis" model. Water Resources and Industry 7: 38-48. https://doi.org/10.1016/j.wri.2014.10.003

Giddings L, Soto M, Rutherford B, Maarouf A. 2005. Standardized precipitation index zones for Mexico. Atmósfera 18 (1): 33–56.

Jierula A, Wang S, Oh TM, Wang P. 2021. Study on accuracy metrics for evaluating the predictions of damage locations in deep piles using artificial neural networks with acoustic emission data. Applied Sciences 11 (5): 2314. https://doi.org/10.3390/app11052314

Kingma DP, Ba JL. 2015. Adam: A method for stochastic optimization. *In* Third International Conference on Learning Representations ICLR, 2015. Cornell University Press: Ithaca, NY, USA, pp: 1–15. https://doi.org/10.48550/arXiv.1412.6980

Kharin VV, Zwiers FW, Zhang X, Hegerl GC. 2007. Changes in temperature and precipitation extremes in the IPCC ensemble of global coupled model simulations. Journal of Climate 20 (8): 1419–1444. https://doi.org/10.1175/JCLI4066.1

Koudahe K, Kayode AJ, Samson AO, Adebola AA, Djaman K. 2017. Trend analysis in Standardized Precipitation Index and Standardized Anomaly Index in the context of climate change in Southern Togo. Atmospheric and Climate Sciences 7 (4): 401–423. https://doi.org/10.4236/acs.2017.74030

McCulloch WS, Pitts W. 1943. A logical calculus of the ideas immanent in nervous activity. The Bulletin of Mathematical Biophysics 5 (4): 115–133.

Magallanes-Quintanar R, Blanco-Macías F, Galván-Tejada EC, Galván-Tejada JI, Márquez-Madrid M, Valdez-Cepeda RD. 2019. Negative regional Standardized Precipitation Index trends prevail in the Mexico's state of Zacatecas. Terra Latinoamericana 37 (4): 487–499. http://dx.doi.org/10.28940/terra.v37i4.563

Mahfouz P, Mitri G, Jazi M, Karam F. 2016. Investigating the temporal variability of the standardized precipitation index in Lebanon. Climate 4 (2): 27. https://doi.org/10.3390/cli4020027

Masinde M. 2014. Artificial neural networks models for predicting effective drought index: factoring effects of rainfall variability. Mitigation and Adaptation Strategies for Global Change 19 (8): 1139–1162. https://doi.org/10.1007/s11027-013-9464-0

McKee TB, Doesken NJ, Kleist J. 1993. The relationship of drought frequency and duration to time scales. *In* Proceedings of the 8th Conference on Applied Climatology, American Meteorological Society: Boston, MA, USA, pp. 179–183.

Naresh Kumar M, Murthy CS, Sesha Sai MVR, Roy PS. 2009. On the use of Standardized Precipitation Index (SPI) for drought intensity assessment. Meteorological Applications 16 (3): 381–389. https://doi.org/10.1002/met.136

Ozger M, Mishra AK, Singh VP. 2011. Estimating Palmer Drought Severity Index using a wavelet fuzzy logic model based on meteorological variables. International Journal of Climatology 31 (13): 2021–2032. http://dx.doi.org/10.1002/joc.2215

R Core Team. 2020. R: A language and environment for statistical computing. R Foundation for Statistical Computing, Vienna, Austria. https://www.cran.r-project.org/ (Retrieved: December 2021).

Sharma S, Sharma S, Anidhya A. 2020. Activation functions in neural networks. International Journal of Engineering Applied Sciences and Technology 6 (12): 310–316. http://dx.doi.org/10.33564/IJEAST.2020.v04i12.054

Soh YW, Koo CH, Huang YF, Fung KF. 2018. Application of artificial intelligence models for the prediction of standardized precipitation evapotranspiration index (SPEI) at Langat River Basin, Malaysia. Computers and Electronics in Agriculture 144: 164–173. https://doi.org/10.1016/j.compag.2017.12.002

Usman SU, Abdulhamid AI, Sawa BA, Kibon AU, Yusuf YO. 2014. An assessment of temporal variability of drought in Katsina using standardized precipitation index. International Journal of Humanities, Arts, Medicine and Sciences 2 (7): 33–40.

Wang W, Van Gelder PH, Vrijling JK, Ma J. 2006. Forecasting daily streamflow using hybrid ANN models. Journal of Hydrology 324 (1–4): 383–399. https://doi.org/10.1016/j.jhydrol.2005.09.032